Diabetic Complications Consortium

Application Title: Quantifying Structural Changes in the Diabetic Foot using Three-dimensional Ultrasound

Principal Investigator: William R. Ledoux, PhD

1. Project Accomplishments:

Volumetric ultrasound scans were taken of the entire plantar soft tissue of four subjects (1 diabetic, 3 nondiabetic) in unloaded, unloaded shear wave elastography, and dual support loaded conditions. Plantar pressure and computed tomography scans were also acquired for validation and stiffness measurements. Loaded and unloaded scans were registered and internal deformations were measured using commercial digital volume correlation software. Vertical displacement, axial and principal strains, and tissue thickness were measured. Tissues were segmented from weighted ultrasound scans to obtain tissue-specific measurements and vertical displacement was registered to plantar pressure to obtain a stiffness map. Ultrasound thickness measurements and volume reconstruction were validated using computed tomography. Ultrasound volume measurements were 11-28% lower than computed tomography measurements. Plantar pressure, average shear wave speed and modulus measurements, and muscle volume measurements were comparable to prior work. Strain maps varied between subjects but demonstrated increased vertical strain in load bearing regions of the fat and skin, higher sagittal shear strain below the metatarsals and lower beneath the calcaneus in the fat and skin, and higher sagittal shear strain at the anterior plantar fascia. Stiffness was highest at the heel and metatarsals and values with within ranges of prior work using similar methods.

2. Specific Aims:

> **SA1)** Develop a mechanical system and the necessary software to generate a three-dimensional scan of the entire plantar soft tissue, using B-mode ultrasound for structural information and shear wave elastography for tissue properties.

The goal of this work is to develop an ultrasound-based method to acquire three-dimensional scans of the plantar soft tissue in both unloaded and naturally loaded states and using both imaging B-mode and shear wave elastography (SWE) modes. A mechanical scanning apparatus was constructed using a stiff, acoustically translucent load-bearing plate and an x-y scanning axis. A software system was developed to control the scanner, record subject and scan information, and reconstruct acquired ultrasound images and shear wave speed values into a volume. An anatomically realistic phantom was developed to aid the evaluation and development of the scanning system. The resulting system is capable of producing volumetric plantar soft tissue scans in both B-mode and SWE with resolution on par with existing volumetric medical imaging systems.

Hardware and Construction
The final design of the scanner frame is constructed from 1.5” aluminum t-slot rail, and the dimensions of the frame are 4’ x 3’ x 3’.

Finite Element Analysis
Once the design was drafted in CAD software, the model was simplified so that finite element analyses could be performed to ensure that the dimensions and materials were acceptable for the anticipated weights to be supported. In particular, the thickness of the sonolucent plate affects the quality of ultrasound images, therefore, the optimal plate is the thinnest plate capable of withstanding loading. The simplified model consisted of just the 1” high density polyethylene (HDPE) plate supported by 1” square hollow tube supports and supporting 1 7/8” aluminum speed rail railings. The HDPE plate had two rectangular cutouts. Both cutouts had a 0. 5” wide, 0.3” thick lip. In the left cutout was a ¼” HDPE plate which was connected to the thicker HDPE plate with a sliding contact. The right cutout contained a water bath with 0.4” thick bottom and 0.5” thick sides connected to the thicker HDPE plate with a bonded contact. All other contacts were defined as bonded and the four rectangular supports were defined as fixed to the ground. A 1334N (300lb equivalent) force was applied to the left thinner plate, and a 677N (150lb equivalent) force was applied to the right plate.

The maximum von mises stress within the thinner, sliding HDPE plate was 3.7MPa, which is 8x lower than the yield strength. The maximum von mises stress within the aluminum was 18MPa, which is 15x lower than the yield stress. The maximum displacement was 4.5mm in the thinner HDPE plate at the location of load application. However, the maximum principal stress was 0.3%, indicating that the sliding contact is likely related to the displacement. The displacement of the section between the two cutouts was 1.53mm, and the first principal strain was .06%. The maximum magnitude of lateral displacement was .0046” (A-P) -0.009” (M-L) in the thinner sliding plate, which is far below the 0.5” wide lip.

Motor and actuator sizing
When designing a motion application, the choice of motors and linear actuators is governed by parameters like resolution, accuracy, speed, load, and orientation. This application involves two perpendicular horizontal axes, with a load that is primarily normal to the direction of motion. The horizontal axes are less complex and require fewer engineering controls than a vertical axis, making this unlikely to be a limiting factor. The load carried by the top axis is comprised of the ultrasound transducer, the transducer housing, and the components that connect the transducer to the actuator. The anticipated load for the longitudinal axis of 587g or 1.2lb is relatively small, which means it likely will not be a limiting factor. Similarly, while the addition of the weight of the longitudinal axis increased the anticipated load for the transverse axis to 787.2g, this load is still relatively small relative to typical applications. Typical resolution of other volumetric medical imaging systems is approximately 0.3mm. In order to image a large foot, the total span of the motion needed to be approximately 320mm in the anterior-posterior direction and 230mm in the medial-lateral direction. This combination of resolution and span is a limiting factor in the choice of linear actuators. Additionally, accuracy and precision are of importance for a research medical imaging motion application, as the true anatomy is the primary output of interest. High resolution and accuracy over a long span is a limiting factor.

Finally, the number and type of scans that can be taken are limited by the speed at which the motion control system can be operated. In order to obtain a high quality image and to have confidence in the reconstruction of the volume, the motion should stop while the image is being acquired. Given that an image acquisition via the research interface takes approximately 0.04 s, the minimum scan time for the maximum scan is: 320mm/0.3mm x 3 passes x 0.04 s/pass = 128s / 60 min = 2.1 min.

Actuator

As a result of the requirements for high precision, accuracy, and repeatability and quick acceleration and deceleration; in combination with the low load, a 1mm lead, 10mm diameter lead screw was chosen with a constant-force anti-backlash nut (CSLSM10AHXR1ZF-2LT-0240-0 and CSLSM10AHXR1ZF-2LT-0440-0, PBC Linear, Roscoe, IL,USA). This actuator uses a recirculating ball bearing between the carriage and the rail which has a static coefficient of friction of 0.02-0.025 and a dynamic coefficient of friction of <0.01.

Motor

The required minimum torque of the motor was calculated using the diameter, length, lead, efficiency, and material of the lead screw, along with the load, acceleration, deceleration, maximum speed, and stopping accuracy. Based on these parameters and a factor of safety of 2, the estimated required torque was 0.26 Nm or 36.7 oz-in. Using this information the NEMA17-16-06PD-AMT112S (CUI devices, Lake Oswego, OR, USA) was selected for both axes. It is rated to 40-25oz-in for speeds from 3000 to 4000 pulses per second with an accuracy of 0.2 degrees.

Top Surface

The top surface of the scanner needs to be strong and stiff enough to support the weight of the lower limb alone for the unweighted scans as well as ½ body weight for the weighted scan without buckling to allow for linear translation of the transducer on the bottom surface. The material also needs to allow sufficient transmission of sound waves to allow both B-mode imaging and shear wave elastography. In order to match sonic properties, the speed of sound and density of a variety of materials was compared with those of various biological tissues, and 8 materials were selected for testing. Parameters such as speed of sound, acoustic power, focal depth, dynamic range, total gain, and time gain compensation were adjusted to obtain the best image. The materials that yielded the best images in B-mode were subjected to SWE imaging. Again, B-mode and SWE parameters were adjusted to obtain the best signal in the phantom area. High density polyethylene (HDPE) was able to acquire good signal in B-mode and SWE. A 1/4" HDPE plate was chosen for loaded scanning. The plate chosen for thinner scans was 1/8" HDPE.

Transducer housing

While the top surface is designed with sufficient stiffness to prevent excessive bending and failure, the plate material best suited to ultrasound imaging and SWE acquisition will likely undergo some bending. This bending may be sufficient to alter the ultrasound signal (via additional compression in areas under more load) or damage the transducer elements. In order to both protect the transducer and ensure that ultrasound signal is as consistent and high-quality as possible, the housing to connect the transducer to the longitudinal linear actuator was designed to respond to increased pressure due to bending. An additional requirement was the need to protect

the transducer cord from excessive bending or force. The final housing is comprised of four pieces: the housing, the sheath, the interface part, and the topper. The custom designed parts were printed in PLA on an Ultimaker S5+.

Electrical

The electrical system consisted of the motor, encoder, printed circuit board, power supply, and a circuit breaker.

Final constructed scanner

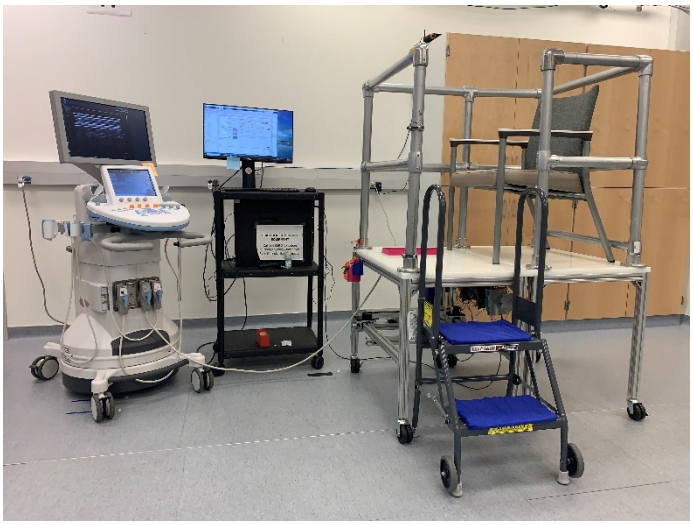

Figure 1: The final constructed scanner including both mobile halves secured together, a set of stairs with handles, motors, linear actuators, and DIN rail mounted electrical system, HDPE plate and water bath, and a chair for the subject to sit on during unweighted data collections.

The final constructed scanner comprised of two linear actuators secured perpendicular to each other using a manufacturer-provided mount, each of which is attached to a stepper motor via a 4mm diameter set screw flexible shaft coupling. The actuators are secured to the t-slot frame using custom-designed parts printed on a Stratasys F370 in acrylonitrile styrene acrylate (ASA). This scanning mechanism is mounted on the t-slot frame, using additional custom-designed parts printed in ASA. The surface of the scanner is one inch thick HPDE. A 14.5” x 8.75” window with a 0.5” lip was milled into the HDPE at 3.5” from the front and 6” from the right side of the plate to allow attachment of an interchangeable thinner HDPE pane for imaging. Four holes were drilled into the lip, on in each corner such that ¼-20 fasteners could be used to further secure the interchangeable plates. Finally, aluminum safety rail was added around the perimeter of the scanner to create a more secure environment for subject safety and comfort. The safety rail was secured through the HDPE plate and directly into the t-slot frame. The scanner was made from two parts and mounted on locking wheels for improved mobility, as it was designed be used and stored in different areas. The 8 legs of the t-slot frame were fitted with 3” rubber caster wheels which were secured directly to the center hollow of the t-slot rail. The two sides of the scanner lock together using a custom designed locking pin mechanism mounted to the t-slot legs. A DIN rail system designed to hold the electrical system was mounted to the t-slot rail using custom designed pieces printed in ASA. The DIN rail system was attached to the front half of the scanning platform for proximity to the motors.

Software

The scanner hardware involves several different components that must be controlled in the appropriate order at regulated time intervals, necessitating custom automation software. In particular, the ultrasound image acquisition and the motor linear translation should be synched to allow image acquisition at regular intervals and allow for easier image reconstruction. The

Aixplorer has an available research package that allows direct image acquisition through a MATLAB interface, making MATLAB the ideal choice for a control software despite its lack of real-time processing. Therefore, an image acquisition graphical user interface (GUI) was developed in MATLAB to perform the scanner control (Figure 2). The user interface contains five sections: subject demographics and test information, quality control checks, imaging parameters, a digital motor positioning system, a scan time estimator, and safety features.

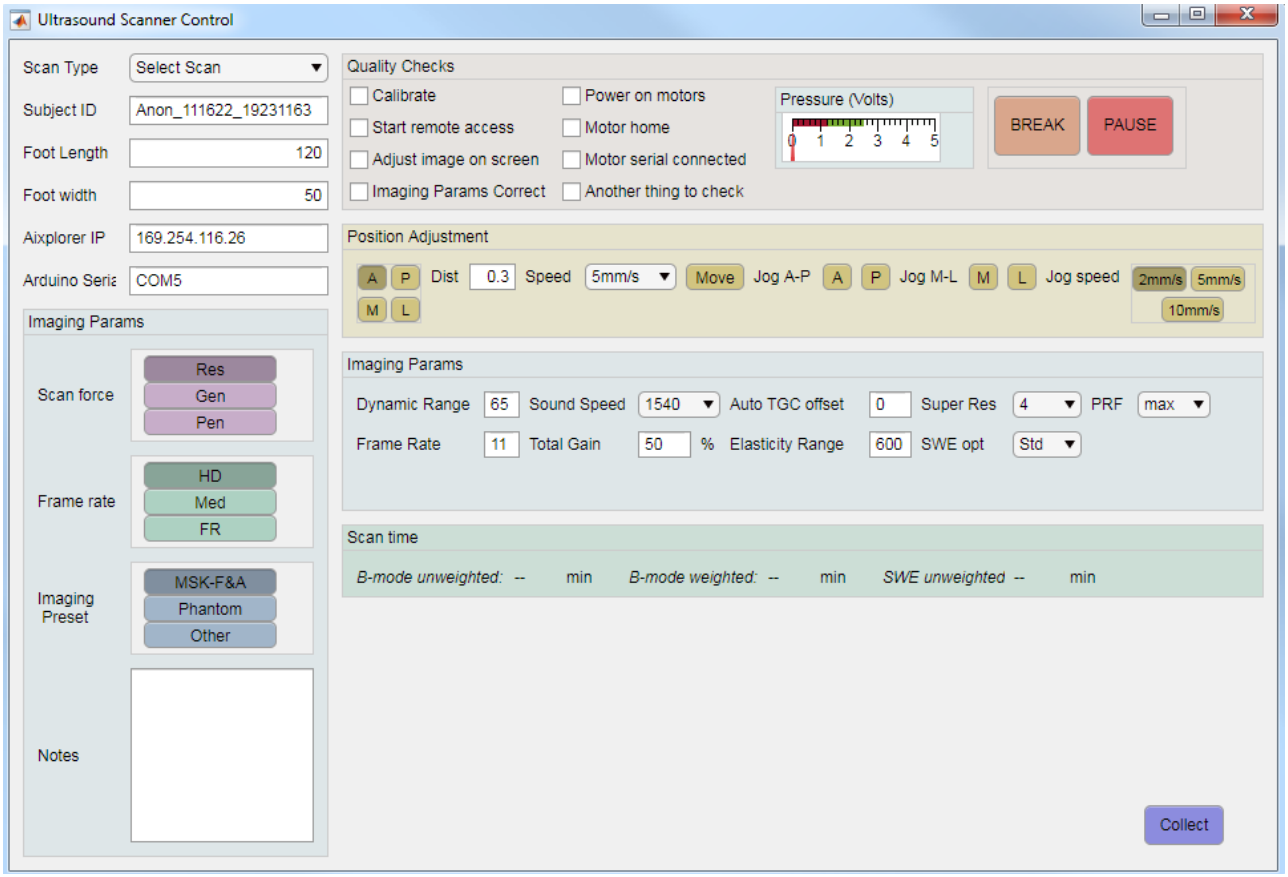

Figure 2: The Graphical User Interface through which the operator interacts with the scanning software during collection of a volumetric ultrasound scan.

> **SA2)** Collect plantar soft tissue scans for 7 diabetic non-neuropathic subjects and 7 non-diabetic subjects.

To address **SA2**, the volumetric scanner was used to collect loaded, unloaded, and SWE scans for 3 non-diabetic and 1 diabetic subject. While this is fewer subjects than initially intended, and the sample size is too small to draw meaningful inference about population differences, the methods developed will enable additional future data collection with minimal startup time.

Introduction

In aim of this work is to develop methods to better understand the multidimensional strain behavior of the plantar soft tissue using a novel load-bearing volumetric ultrasound device capable of obtaining loaded and unloaded volumetric images of the entire plantar soft tissue. Volumetric ultrasound scans were taken of the entire plantar soft tissue of four subjects (1

diabetic, 3 nondiabetic) in unloaded, unloaded shear wave elastography, and dual support loaded conditions. Plantar pressure and computed tomography scans were also acquired for validation and stiffness measurements. Loaded and unloaded scans were registered and internal deformations were measured using commercial digital volume correlation software. Vertical displacement, axial and principal strains, and tissue thickness were measured. Tissues were segmented from weighted ultrasound scans to obtain tissue-specific measurements and vertical displacement was registered to plantar pressure to obtain a stiffness map.

Demographics

Six (D=3, ND=3) age-matched subjects were recruited for this IRB-approved protocol (2 were later excluded). Subjects were ambulatory, and those with neuropathy, recent injury to the lower limb, diagnosed peripheral vascular disease, or arthritis were excluded. Hba1c was recorded from the last clinical visit on record when applicable.

Initial protocol

Subjects first had measurements of height and weight taken. Then, subjects underwent a 10g (5.07) Semmes Weinstein monofilament test for sensation. Subjects who were not able to accurately locate the 10 contact sites of the monofilament were excluded from the study. Measurements of foot length and width were recorded in order to set scanning parameters. Finally, subjects were asked to walk across a 6m path four times a normal speed to obtain the subjects normal self-selected walking speed.

Plantar pressure

Plantar pressure data was taken using the novel emed plantar pressure platform. Three to five trials each of static plantar pressure and dynamic plantar pressure were recorded for each foot. Dynamic trials were captured at a self-selected walking speed that matched previously recorded typical walking speed for each subject. Plantar pressure was automatically masked using the novel 10-region mask, and peak plantar pressure and pressure-time integral (PTI) were extracted from the multimask software.

Ultrasound Scans

After plantar pressure collection, subjects were seated on the ultrasound scanning machine (Figure 3). The right foot was placed either in an isotonic (0.9% NaCl) water bath or on a custom polyacrylamide hydrogel coupling pad. In the case of polyacrylamide hydrogel pads, they were manufactured according to an in house developed protocol and within 2 hours of data collection, were removed from the CaCl storage solution, washed, and stored in an isotonic NaCl and glycerin solution to reduce irritation and drying associated with prolonged skin contact. The transducer was coupled to the underside of the plate using either a hydrogel burn pad secured with a polyurethane adhesive bandage, or a custom molded polyacrylamide hydrogel couplant. Unweighted structural scans were taken with B-mode ultrasound through a 1/8” HDPE plate using an SL18-5 transducer and an Aixplorer (Supersonic Imagine, Aix-enProvonce, France) using the MSK Foot & Ankle preset, 1660 m/s, Res (C1) or Pen, and HD. The images were taken with 0.3925 mm- 0.474mm spacing in the anterior-posterior direction. Subjects were instructed to relax their foot and hold it still. After the unweighted structural scans, an unweighted material scan was taken using shear wave elastography and 1.5mm-2.5mm spacing in the anterior-posterior direction. The SWE focus for the SWE images was set just deep to the superior extent

of the SWE box. The SWE box was set to the maximum size allowed and positioned on the medial side of the image to allow overlap of SWE values. Three SWE images were taken at each step to allow the SWE signal to stabilize, based on previously reported reliability testing. Weighted structural scans were taken with B-mode ultrasound through a 1/4" HDPE plate. The structural scans took 9-10 minutes to complete depending on the length of the foot while the SWE scan took between 14-30 minutes to complete. In total 2 unweighted structural scans, one SWE scan, and one weighted structural scan were acquired. Subjects dried off their foot and rested it outside the scanning area between scans for between 5 and 15 minutes. Subjects typically took a break including walking around the test area between the unweighted and weighted scans as this required changing the scanner plate.

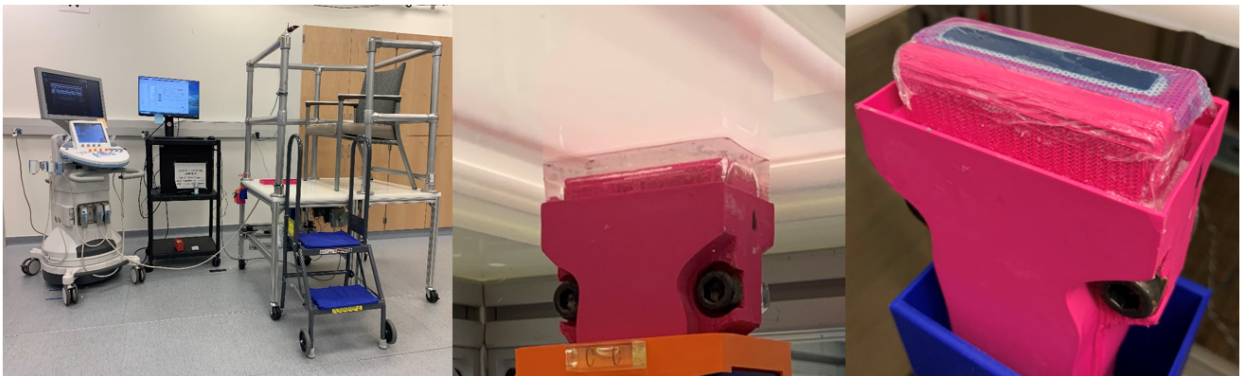

Figure 3: Left: setup for volumetric ultrasound scans. Subjects ascend the stairs and either sit in the chair or stand placing equal weight in the scanning area and the non-scanning area. The computer hosts the MATLAB-based control program and the system uses an Aixplorer commercial ultrasound machine.

CT

A computed tomography (CT) scan was taken using the CurveBeam Lineup (Hatfield,PA,USA) using the large field of view, small (C1) or standard patient preset, which uses 100kV (small) or 120kV (standard) and 5mA. In all, 17 bones (calcaneus, 5 metatarsals, 3 cuneiforms, cuboid, navicular, 5 phalanges, and sesamoids) were manually segmented from the right foot to use for validation of the thickness measurements as well as to automatically mask the plantar pressure measurements.

Ultrasound image registration and volume reconstruction

Ultrasound images were registered within-scan manually using a custom-developed graphical user interface (GUI). This user interface allows a user to align the images using different horizontal overlaps, vertical displacements, and rotations. It also allows the user to incrementally adjust the image anterior-posteriorly between the three passes of the scan in the case of movement or motor stalling. After manual medial-lateral registration, the scans were registered anterior-posteriorly between steps using normalized cross correlation to offset minor movements during the scan. The images were stitched by taking the maximum value of the image intensity in overlapping regions and normalized by the maximum intensity per column.

Shear wave elastography images were reconstructed by first registering the blue channel of the saved live screen images in the same manner as the B-mode scans. Then, the raw shear wave

speed (SWS) values saved from the research interface were positioned inside an empty matrix according to the SWE box size, image size, and SWE box position information saved from the research interface. SWS values outside of the expected range based on the maximum rated modulus were removed and SWS matrices were up sampled to the resolution of the images using nearest neighbor interpolation prior to placement in the image area. A composite SWS map was created by taking the per-pixel average of the 3-4 SWS acquisitions taken at each step. Then the registration determined from the image data was used to reconstruct a volume of SWS values.

Registration between scans of different types was performed manually using point-to-point registration in 3D Slicer. Points chosen included metatarsal heads, the base of the fifth metatarsal, and the inferior calcaneus for translation and rotation in the transverse, coronal, and sagittal planes, and the scanning plate for translation along the superior-inferior axis. Ultrasound volumes were registered so that the scanning plates were aligned. The transform estimated from slicer was transferred to MATLAB and used to transform the volumes before saving the file format required for digital volume correlation (DVC).

DVC

Registered weighted and unweighted ultrasound volumes were resized to a cubic voxel in MATLAB using built in function interp3 with the cubic method. Resized volumes were imported into StrainMaster digital volume correlation software (LaVision, Ypsilanti, MI). After determining best parameters, displacement and strain along each anatomical axis, shear strain in each anatomical plane, principal strains, and the correlation value quality metric were exported from the software as a .dat file for subsequent analysis in MATLAB.

Segmentation

All visible intrinsic muscles, skin, plantar fat, visible bones, general soft tissue, and the scanning plate were manually segmented from the weighted scans, and soft tissues of interest for SWE analysis were manually segmented from unweighted scans using Mimics (Materialise). All foot bones and the load bearing plate were segmented from CT scans using thresholding tools available in Mimics.

Muscle Volume

Muscle volumes were measured using the regionprops3 function in MATLAB on the label matrix defined by the segmented weighted volume and converted from voxels to cm^3 using the scan resolution.

Deformation

Displacement, strain, and correlation values were reconstructed from the coordinate-value output file into a volume of the same size as the segmented volume of the weighted scan using the input resolution of the volumes. Mask volumes for each tissue were created from the segmented volume, and masks were applied to the deformation values and average and maximum values were taken for each tissue along the inferior-superior axis to create maps in the transverse plane. The deformation and strain volumes were also colorized and overlaid on sliced from the weighted volume using custom MATLAB code.

Stiffness
Vertical displacement and average vertical force were calculated from DVC and plantar pressure values, respectively. Vertical displacement was taken as the maximum vertical displacement along the superior-inferior axis across the 3D spatial locations within the segmented soft tissue volume. Force was calculated as the average of all force values in a single spatial sensor location over the duration of a static pressure acquisition between the cutoff for step-on frames and the last frame, where force is the pressure multiplied by the sensor area.

> **SA3)** Analyze these scans using segmentation and strain information calculated with digital volume correlation (DVC) as well as an interpretable classification neural network.

To address **SA3**, the loaded and unloaded scans were processed using digital volume correlation and displacement and normal and shear strain were extracted for the three anatomical axes. Scans were compared to computed tomography to assess the accuracy of measurements through the acoustically transparent plate, displacements were correlated with plantar pressure to obtain regional stiffness maps, and scans were segmented to obtain tissue-specific strain and SWE values as well as to assess tissue morphology. While the sample size was insufficient to process scans using the neural networks proposed, the development of the analysis methods described allow future work using volumetric ultrasound scans to be directly compared to prior work and expands prior measurements into two (stiffness) or three (modulus, strain) dimensions. The introduction of additional dimensions to previously devised measurements allows interrogation of previously unmeasured quantities and the evaluation of long-standing hypothesis about the mechanical etiology of plantar ulceration.

Ultrasound thickness measurements and volume reconstruction were validated using computed tomography. Ultrasound volume measurements were 11-28% lower than computed tomography measurements. Plantar pressure, average shear wave speed and modulus measurements, and muscle volume measurements were comparable to prior work. Strain maps varied between subjects but demonstrated increased vertical strain in load bearing regions of the fat and skin, higher sagittal shear strain below the metatarsals and lower beneath the calcaneus in the fat and skin, and higher sagittal shear strain at the anterior plantar fascia. Stiffness was highest at the heel and metatarsals and values with within ranges of prior work using similar methods.

Data collection
As a result of variations in ultrasound parameters, data collection protocols, subject motion, and exclusion criteria, data quality varied between subjects. As a result, not all of the data was analyzed for all subjects.

Volume validation
Bone to plate distances measured from ultrasound volumes were 9-28% lower than those measured from the corresponding CT. Errors for subjects C2 and C3 were lower than for C1.

Plantar pressure
Dynamic peak pressure, pressure time integral, and force time integral for the 4 subjects were measured. Peak values for all static variables and dynamic trials occurred at the heel. However,

peak overall pressure occurred at the hallux for two subjects and the heel and fifth metatarsal head for the two other subjects. The maximum pressure gradient occurred at the forefoot for two control subjects and at the fifth metatarsal head for the remaining control and diabetic subject. The maximum pressure gradient angle occurred at the metatarsal heads for all subjects. Differences between groups were minimal. The single subject with diabetes demonstrated less variability across regions in temporal integral variables but a larger difference between regions in maximum pressure gradient angle.

Segmentation

The scanning plate, 11 bones, and 10 soft tissue structures were successfully segmented from the weighted ultrasound scan of C2, and a subset of those were segmented from the weighted and unweighted scans of other subjects (Figure 4). All soft tissue not readily identifiable as one of the 10 structures was labeled as a general soft tissue (only pictured in the coronal overlays). The 3D model of the weighted segmentation for subject C2 is displayed.

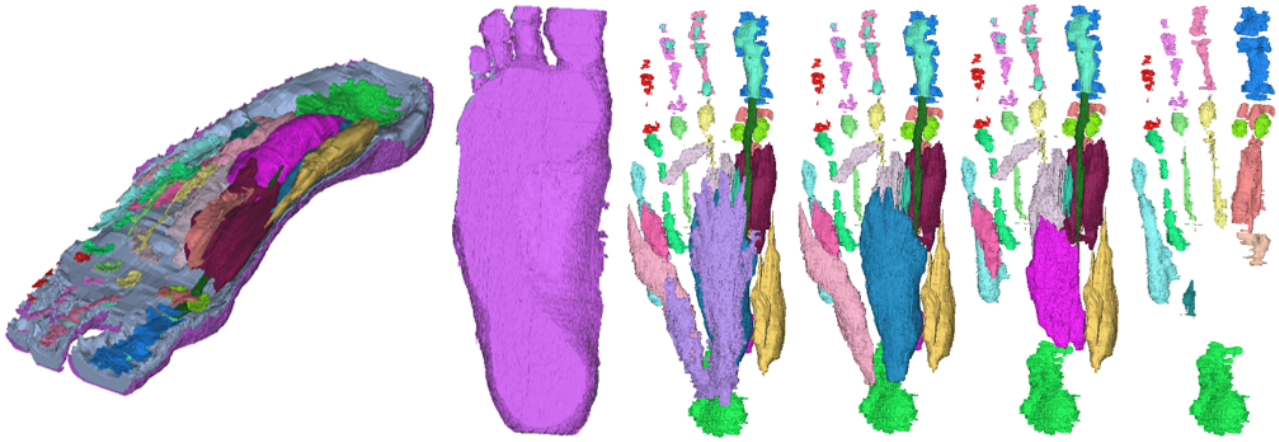

Figure 4: 3D rendering of segmented tissues from subject C2. Left: orthogonal view of all segmented tissues. Right: superficial to deep layers of plantar fascia and muscles.

Muscle Volume

Fewer muscle volumes were segmented for subject C1 than C2. Of the muscles and soft tissues present in both segmentations, the skin, adipose, plantar fascia, and total soft tissue volume were larger in subject C1 than subject C2.

SWE

SWS values calculated from each tissue were determined for 3 subjects. The shear wave speed and modulus were generally lower in the toes and midfoot and higher on the relatively higher load bearing forefoot (metatarsal heads) and hindfoot. This pattern was most clearly visible in the fate and less pronounced in the skin. The signal in the plantar fascia was too poor to obtain meaningful values. Differences between control subjects (C1,C2) were larger than differences between diabetic (D1) and control subjects. Standard deviations for all values were similar to or larger than mean values.

DVC, Deformation and Stiffness

Average axial and shear strains for all three axes, average maximum principal strain, and average vertical displacement for all fat and skin were calculated. Similar maps for additional tissues can be found in the supplemental images. There were large variations in strain and displacement patterns between subjects. Strain maps from both subjects demonstrated negative vertical strain along the primary load bearing locations (metatarsal heads, lateral midfoot, and heel) of the fat and skin, higher sagittal shear strain at the submetatarsal fat and skin, lower sagittal shear strain at the subcalcaneal fat and skin, and higher sagittal shear strain in the distal plantar fascia. Within the flexor digitorum brevis, there was an anterior-medial gradient of vertical displacement in both subjects, with higher magnitude displacement at the posterior-lateral end and lower magnitude displacement at the anterior-medial side. The measured stiffness was around 0.5 N/mm, with higher values in the heel and metatarsal heads and noise particularly on the lateral edge of the foot (Figure 5).

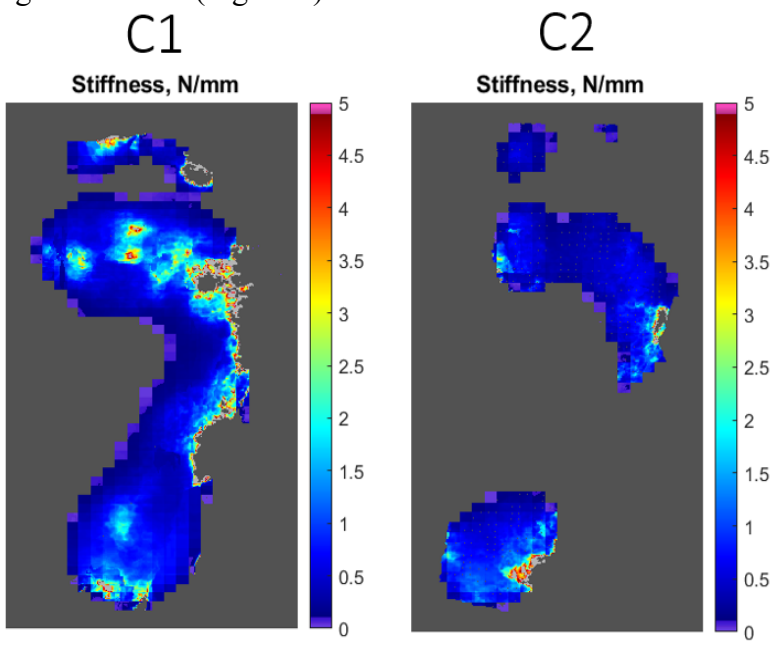

Figure 5: Spatial stiffness heat maps calculated from DVC-based deformation and registered plantar pressure.

3. Publications:

There are currently no publications from this work as it is still in progress.